

Layanan Perpustakaan UHAMKA

1-s2.0-S2667031326000229-main (1)

 23 April 2026

Document Details

Submission ID

trn:oid::3618:139157538

Submission Date

May 16, 2026, 8:40 AM GMT+7

Download Date

May 16, 2026, 8:53 AM GMT+7

File Name

1-s2.0-S2667031326000229-main (1).pdf

File Size

16.2 MB

13 Pages

8,865 Words

50,512 Characters





15% Overall Similarity

The combined total of all matches, including overlapping sources, for each database.




Exclusions

▸ 52 Excluded Matches

Match Groups

-  **24 Not Cited or Quoted 6%**
Matches with neither in-text citation nor quotation marks
-  **3 Missing Quotations 2%**
Matches that are still very similar to source material
-  **15 Missing Citation 7%**
Matches that have quotation marks, but no in-text citation
-  **0 Cited and Quoted 0%**
Matches with in-text citation present, but no quotation marks

Top Sources

- 11%  Internet sources
- 14%  Publications
- 11%  Submitted works (Student Papers)

Integrity Flags

0 Integrity Flags for Review

Our system's algorithms look deeply at a document for any inconsistencies that would set it apart from a normal submission. If we notice something strange, we flag it for you to review.

A Flag is not necessarily an indicator of a problem. However, we'd recommend you focus your attention there for further review.

Match Groups

- **24 Not Cited or Quoted 6%**
Matches with neither in-text citation nor quotation marks
- **3 Missing Quotations 2%**
Matches that are still very similar to source material
- **15 Missing Citation 7%**
Matches that have quotation marks, but no in-text citation
- **0 Cited and Quoted 0%**
Matches with in-text citation present, but no quotation marks

Top Sources

- 11% Internet sources
- 14% Publications
- 11% Submitted works (Student Papers)

Top Sources

The sources with the highest number of matches within the submission. Overlapping sources will not be displayed.

| | | | |
|----|----------------|---|-----|
| 1 | Publication | Irena Ujjanti, Mulyoto Pangestu, Thomas Mayers, Wawang S Sukarya et al. "Evalu... | 8% |
| 2 | Student papers | Gauhati University on 2026-05-08 | 1% |
| 3 | Publication | Irena Ujjanti, Bety S Lakhsmi, Zahra Nurushoffa, Wawang S Sukarya, Supandi, Ta... | <1% |
| 4 | Internet | jurnal.stikes-ibnusina.ac.id | <1% |
| 5 | Student papers | Academic Library Consortium on 2024-06-11 | <1% |
| 6 | Student papers | University of Pretoria on 2025-08-12 | <1% |
| 7 | Student papers | Monash University on 2026-05-03 | <1% |
| 8 | Publication | Fengli Guan, Shuancheng Zhang, Lijie Fan, Ying Sun, Yucong Ma, Can Cao, Yu Zha... | <1% |
| 9 | Internet | www.mdpi.com | <1% |
| 10 | Publication | Alexia Omont, Milton Spanopoulos-Zarco, Juan Manuel Pacheco-Vega, Alberto Pe... | <1% |

| | | | |
|----|----------------|--|-----|
| 11 | Internet | liulin.nankai.edu.cn | <1% |
| 12 | Publication | Yuan Meng, Xiaojuan Xu, Dong Niu, Yangjie Xu, Yanling Qiu, Zhiliang Zhu, Hua Zh... | <1% |
| 13 | Internet | www.snoco.org | <1% |
| 14 | Internet | journals.biologists.com | <1% |
| 15 | Publication | Irena Ujianti, Mulyoto Pangestu, Thomas D Mayer, Wawang S Sukarya et al. "Eval... | <1% |
| 16 | Publication | Bayo Olufunso Adeoye, Oyedayo Phillips Akano, Oluwatoyin Michael Daniyan, Pe... | <1% |
| 17 | Student papers | University of KwaZulu-Natal on 2024-02-06 | <1% |
| 18 | Student papers | Krida Wacana Christian University on 2023-04-23 | <1% |
| 19 | Internet | www.frontiersin.org | <1% |
| 20 | Student papers | NHS National School of Healthcare Science on 2025-08-16 | <1% |
| 21 | Internet | ouci.dntb.gov.ua | <1% |
| 22 | Internet | www.chemspider.com | <1% |
| 23 | Student papers | ebsu on 2022-12-09 | <1% |
| 24 | Internet | webbook.nist.gov | <1% |

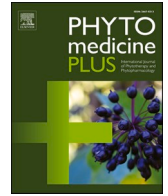
| | | | |
|----|----------------|---|-----|
| 25 | Student papers | University of Huddersfield on 2026-04-08 | <1% |
| 26 | Publication | Qi Han, Xiao Gao, Shuwei Wang, Zhaolan Wei, Yunyi Wang, Ke Xu, Mingqing Chen.... | <1% |
| 27 | Publication | Novadri Ayubi, Dyah Fitria Padmasari, Atika Syafawi, Deby Tri Mario et al. "Potent... | <1% |
| 28 | Internet | repository.uhamka.ac.id | <1% |



Contents lists available at ScienceDirect

Phytomedicine Plus

journal homepage: www.sciencedirect.com/journal/phytomedicine-plus



Evaluating the effects of sea cucumber extract supplementation on the developmental competence of aged oocytes during *in vitro* fertilization and *in vitro* maturation

28 Irena Ujianti^{a,*}, Mulyoto Pangestu^b, Thomas Mayers^c, Wawang S Sukarya^d, Bety Semara Lakhsmi^e, Zahra Nurushoffa^f, Supandi^g, Takashi Yashiro^h

- ^a Department of Medical Physiology, Faculty of Medicine, Universitas Muhammadiyah Prof. Dr. HAMKA, Jakarta, Indonesia
- ^b Department of Obstetric Gynaecology, Faculty of Medicine, Monash University, Clayton, Australia
- ^c Institute of Medicine, University of Tsukuba, Japan
- ^d Department of Obstetric Gynaecology, Faculty of Medicine, Universitas Muhammadiyah Prof. Dr. Hamka, Jakarta, Indonesia
- ^e Department of Public Health, Faculty of Medicine, Universitas Muhammadiyah Prof. Dr. HAMKA, Jakarta, Indonesia
- ^f Department of Pathology Anatomy, Faculty of Medicine Universitas Muhammadiyah Prof. Dr. HAMKA, Jakarta, Indonesia
- ^g Department of Pharmaceutical Chemistry, Faculty of Pharmacy and Science, Universitas Muhammadiyah Prof. Dr. HAMKA, Indonesia
- ^h Jichi Medical University School of Medicine, Japan

ARTICLE INFO

Keywords:
 Oxidative stress
 Antioxidants
 Embryo development
 HSP90 gene
 GPX1 gene

ABSTRACT

Background: Ovarian aging, characterized by declines in oocyte quantity and quality, results in reduced fertility, particularly in women over 38 years of age. Oxidative stress and endoplasmic reticulum (ER) stress are major contributors, necessitating strategies to support the developmental competence of aged oocytes. *Holothuria lessoni*, a sea cucumber species rich in bioactive compounds, offers antioxidant and cytoprotective potential that may help counteract these oxidative and ER stress-related declines.

Material and methods: Aged oocytes from BL6 hybrid female mice were fertilized *in vitro* and cultured with sea cucumber extract at concentrations of 0, 15, 20, and 25 ppm. Embryo development was evaluated at 24-, 48-, 72-, 96-, and 120-hours post-fertilization. Gas chromatography–mass spectrometry (GC–MS) was used to characterize extract composition, while quantitative reverse transcription polymerase chain reaction (qRT–PCR) of blastocyst expression of HSP90, and GPX1. *In silico* protein–protein interaction and pathway analyses were performed using bioinformatics databases.

Results: GC–MS revealed multiple bioactive constituents, including fatty acids, esters, squalene, and siloxane derivatives. A concentration of 20 ppm yielded the best developmental outcomes, with 100% of embryos reaching the two-cell stage and 29% forming blastocysts, along with superior blastocyst morphology, while 25 ppm reduced embryo quality. At 20 ppm, HSP90 and GPX1 were upregulated 20-fold and 6.58-fold, respectively, whereas 25 ppm further increased GPX1 but decreased HSP90 expression. Network analysis identified TP53, TNF, and IL1B as central regulators in oxidative stress-related pathways.

Conclusions: *Holothuria lessoni* extract at 20 ppm enhanced early embryonic development of aged murine oocytes, likely by modulating oxidative stress and proteostasis via HSF1–HSP90 and Nrf2–GPX1 pathways. Further studies are required to optimize dosing and confirm downstream molecular targets for later developmental stages.

1. Introduction

Ovarian aging represents a progressive decline in both the quantity and quality of oocytes, a process that accelerates markedly after the age

of 38 (Broekmans et al., 2009). In older women, infertility is frequently attributed to a reduced ovarian reserve and diminished developmental competence of oocytes (Wang et al., 2023). These age-related changes contribute to a higher incidence of aneuploidy, impaired oocyte

* Corresponding author at: Faculty of Medicine, Universitas Muhammadiyah Prof. Dr. HAMKA, Jakarta, Indonesia.

E-mail address: irenaujianti@uhamka.ac.id (I. Ujianti).

<https://doi.org/10.1016/j.phyplu.2026.100976>

Available online 6 March 2026

2667-0313/© 2026 The Author(s). Published by Elsevier B.V. This is an open access article under the CC BY license (<http://creativecommons.org/licenses/by/4.0/>).

maturation, increased risk of miscarriage, and lower success rates in assisted reproductive technologies (ART), including *in vitro* fertilization (IVF) (Voros et al., 2025). In parallel, the prevalence of infertility continues to rise, driven by delayed childbearing, chronic psychosocial stress, metabolic disorders, and environmental insults, with substantial consequences for mental health, healthcare utilization, and socioeconomic productivity (Moutzouroulia et al., 2025).

Oocytes are among the most mitochondria-rich cells in the body, reflecting their high adenosine triphosphate (ATP) demand for meiotic maturation, fertilization, and early embryonic development (Ma et al., 2024). With advancing age, mitochondrial efficiency declines, leading to increased electron leakage and overproduction of reactive oxygen species (ROS) (Song et al., 2024). Initially, endogenous antioxidant systems attempt to compensate through the up-regulation of detoxifying enzymes and redox-regulating genes, however, in aged oocytes this compensatory response becomes insufficient. Excess ROS induces oxidative damage to mitochondrial and nuclear DNA, proteins, and membrane lipids, impairing protein folding and activating the unfolded protein response (UPR) (Zhou et al., 2024). Sustained UPR signaling causes prolonged endoplasmic reticulum (ER) stress, during which heat shock proteins such as heat shock protein 90 (HSP90) are mobilized to maintain proteostasis by refolding misfolded proteins (Kunachowicz et al., 2024). Persistent ER stress, together with mitochondrial dysfunction, promotes cellular senescence, disrupts meiotic spindle assembly, increases chromosome segregation errors, and ultimately reduces the developmental competence of aging oocytes (Wang et al., 2025).

Antioxidant-based strategies have therefore been explored to limit oxidative damage and preserve oocyte function (Cao et al., 2022; Hoang Thanh et al., 2022). Marine-derived bioactives, including sea cucumber extracts, have shown promising antioxidant and cytoprotective effects in various experimental models (Ujianti et al., 2025, 2024). Our previous *in vivo* study demonstrated that sea cucumber extract can reduce ROS levels in lipopolysaccharide-induced inflammatory models and modulate adipogenesis and inflammation in adipose-derived stem cells, as well as in obese rodents (Al'asyi et al., 2025). Other studies have reported improved blastocyst formation and embryo quality in IVF and *in vitro* maturation systems using sea cucumber extracts or isolated saponin fractions, particularly in young mouse oocytes (Khalilzadeh et al., 2016; Moghadam et al., 2016). In the context of female reproduction, *in silico* and *in vitro* work has suggested a protective role of sea cucumber extract on reproductive tissues, supported by *in vivo* findings of increased estradiol levels following supplementation (Askari et al., 2024; Maskur et al., 2024). In addition, one of the most crucial molecular chaperones involved in embryonic development is HSP90, particularly the isoform HSP90AA1. HSP90AA1 functions as a key support protein that maintains the proper functioning of multiple critical pathways during oocyte maturation and early embryonic development. In the absence of HSP90AA1, these developmental processes become inefficient and embryo quality is significantly reduced (Zhao et al., 2024). HSP90 also helps counteract the effects of increased ROS by mediating the UPR. This condition leads to elevated HSP90 expression to support the UPR and restore cellular homeostasis (Singh et al., 2025). However, the direct effects of sea cucumber extract on aged oocytes remain poorly characterized, especially regarding oocyte quality, the expression of genes involved in oxidative and ER stress, and subsequent embryo development during IVF. Given the global trend toward delayed childbearing and the rising burden of age-related infertility, there is an urgent need for adjuvant strategies capable of preserving oocyte quality under conditions of heightened oxidative and ER stress. *Holothuria lessoni* (*H. lessoni*), a sea cucumber species rich in bioactive compounds, exhibits antioxidant and cytoprotective properties that may counteract these stress-related declines. Accordingly, the purpose of the current study was to examine, using a murine model, whether *H. lessoni* extract can alleviate oxidative and ER stress in aged oocytes, restore expression of stress-responsive genes such as HSP90 and glutathione peroxidase 1

(GPX1), and enhance oocyte maturation and embryonic developmental outcomes.

2. Materials and methods

2.1. Sample collection and extract preparation

The extraction procedure was adapted from the optimized protocol for isolating secondary metabolites from sea cucumber tissues (Popov et al., 2022). *H. lessoni* specimens were collected in October and November 2024 through daytime diving at Paguyaman Beach, Boalamo, Gorontalo, Indonesia. *H. lessoni*, commonly referred to as the Golden Sandfish, is a species of sea cucumber that is extensively found throughout the Indo-West Pacific region and often inhabits reef flats, coastal lagoons, seagrass beds, and sandflats. Identification was confirmed based on morphological characteristics and reference to relevant taxonomic keys.

To obtain the *H. lessoni* extract, the body wall was separated and cut into segments of approximately 1 cm in size. These segments were thoroughly dried to reduce water content and then subjected to extraction. The dried material was mixed with ethanol at a sample-to-solvent ratio of 1:5 (w/v), facilitating protein breakdown as well as efficient extraction of secondary metabolites. The mixture was incubated under constant agitation to maximize extraction efficiency. Subsequently, the ethanolic mixture was concentrated by rotary evaporation at 40 °C (Heidolph Instruments GmbH, Schwallbach, Germany) to remove residual ethanol and obtain a semi-solid crude extract. The concentrated ethanolic extract was re-dissolved in analytical-grade n-hexane, vortexed for 1 min, and centrifuged at 12,000 rpm for 10 min to remove insoluble residues. The resulting clear supernatant was then filtered through a 0.22 µm PTFE syringe filter to ensure compatibility with the GC-MS system. The concentrate was kept at 4 °C until it was ready for subsequent chemical and biological analyses.

2.2. *H. lessoni* extract characterization

Analysis was conducted using a gas chromatography-mass spectrometry (GC-MS) system (Thermo Fisher Scientific, Chromeleon 7, Version 7.2.10.24543). Chromatographic separation was conducted utilizing an HP-5MS UI capillary column with 30 m length, 0.25 mm internal diameter, and 0.25 µm film thickness. The oven temperature was initially set at 50 °C, held for 2 min, then finally increased to 280 °C, with a total run time of 58 min. The injector was utilized in split mode with a split flow of 50 mL/min as well as an inlet temp of 220 °C. The carrier gas flow was kept at 1.0 mL/min, although the type of carrier gas was not specified, helium or nitrogen is primarily used in similar analyses. An injection volume of 1.1 µL was delivered through a TriPlus RSH autosampler, which used a 10 µL syringe with a needle length of 57 mm. Pre- and post-injection wash cycles were set to 5 cycles to minimize carryover. For mass spectrometric detection, the transfer line temperature was kept at 250 °C as while the ion source temperature was maintained at 200 °C. Electron ionization (EI) was applied in positive polarity mode, and full-scan data were acquired over an *m/z* span of 50–650 at a scan time of 0.2 s. Quantification and identification were conducted using Chromeleon 7 software.

2.3. Medium preparation with sea cucumber extract

H. lessoni extract was first dissolved in phosphate-buffered saline (PBS) to make a 2500 ppm stock solution. This stock was then diluted with medium to obtain working concentrations of 15, 20, and 25 ppm. The control consisted only of medium without added extract. The PBS concentration in the final working solutions was kept below 0.1 % by volume.

2.4. Animal handling

Mice were purchased from Jackson Laboratory (Bar Harbor, ME, USA). Hybrid male mice (C57BL/6 J × BALB/cJ) were used as sperm donors. Hybrid female mice F1 B6D2F1/J (C57BL/6 J × DBA/2 J) and B6CBAF1/J (C57BL/6 J × CBA/J) were used in selected experiments. The mice were kept on a 14-hour light/10-hour dark cycle. Animals were euthanized via cervical dislocation.

2.5. Oocyte collection

BL6 hybrid female mice (C57BL/6 J × BALB/cJ) aged 9–10 months, representing a naturally aged murine model due to their rapidly declining fertility, were used alongside young females aged 6–8 weeks for oocyte collection. The mice were housed in temperature-controlled conditions with a 12-hour dark and 12-hour light cycle, with food and water provided at all times. To collect cumulus–oocyte complexes (COCs), mice received injections of 10 IU equine chorionic gonadotrophin, followed by another 10 IU of HCG from, 48 h later. Fourteen hours after the HCG injection, COCs were collected from the oviductal ampulla as part of the superovulation protocol.

2.6. In vitro fertilisation

In vitro fertilisation of the collected COCs was conducted by incubation with spermatozoa retrieved from the cauda epididymidis of adult male mice, in small drops of fertilization medium with concentration of *H. lessoni* extract. The procedure was carried out under mineral oil and maintained at 37 °C within a controlled gaseous environment comprising 6 % CO₂, 5 % O₂, and 90 % N₂ for 4 h to optimize fertilization outcomes.

2.7. Embryo culture

Embryos were cultured in groups of 10 within 20 µL drops of SAGE 1-Step™ medium with specific concentration of *H. lessoni* extract, placed in 35-mm Petri dishes (Falcon, BD Biosciences) covered by paraffin oil (Ovoil, Vitrolife AB, Sweden), and maintained at 37 °C in 6 % CO₂, 5 % O₂, and 90 % N₂ in a time laps humidified multi-gas incubator (Sanyo MCO-5M[RC], Japan). For the first 24, 48, 72 h, and 120 h, the embryos were assessed for developmental progression.

2.8. RNA extraction and cDNA synthesis

Blastocysts and two-cell-stage embryos were collected following treatment with ethanol extract at concentrations of 0, 15, 20, and 25 ppm. Total RNA from treated and untreated control samples was extracted using the PureLink™ RNA Mini Kit (Cat.: 12183018A, Thermo Fisher Scientific, Waltham, MA, USA), following the manufacturer's instructions. The RNA concentration and purity were assessed with a NanoDrop™ 2000 Spectrophotometer (Thermo Fisher Scientific, Waltham, MA, USA), with acceptable 260/280 nm absorbance ratios defined as 1.8 or higher. For cDNA synthesis, 1 µg of total RNA was reverse transcribed using the ABScript II cDNA First-Strand Synthesis Kit, according to the provided guidelines.

2.9. qRT-PCR analysis

The amplified section for the Caspase-3 gene included part of the 5' upstream region. Primer sequences (Table 1) were obtained from the National Center for Biotechnology Information (NCBI) and designed using online primer-design tools. For glyceraldehyde-3-phosphate dehydrogenase (GAPDH), the forward primer was CATCACTGCCACCCA-GAAGACTG and the reverse primer was ATGCCAGTGAGCTTCCCGTTCAG. For HSP90, the forward primer was TCATTATTCAGGCTGCCGTGGTA and the reverse primer was

Table 1

Representative GC–MS chromatogram of freeze-dried sea cucumber extract.

| No. | Compound Name | Retention Time (min) | Relative Content (%) |
|-----|---|----------------------|----------------------|
| 1 | 2-(4,9,15-Trioxa-3,5,8,10,12,14,16-heptazatetracyclo[11.3.0.0 ² ,0 ⁷ ,11]hexadeca-1(16),2,5,7,10,13-hexaen-12-yl) ethanol | 29.730 | 1.08 |
| 2 | Pyrrolo[1,2-a]pyrazine-1,4-dione, hexahydro- | 30.682 | 3.46 |
| 3 | Cyclodecanone | 30.923 | 6.67 |
| 4 | Propane, 1,2,2-trichloro-1,3,3,3-pentafluoro- | 31.165 | 13.94 |
| 5 | Phthalic acid, hexyl 1-phenyl propyl ester | 31.530 | 5.87 |
| 6 | Citronellal | 31.847 | 3.07 |
| 7 | 3,6-Octadien-1-ol, 3,7-dimethyl-, (Z) | 32.033 | 1.11 |
| 8 | 9-Octadecenoic acid (Z)-, 2,3-dihydroxypropyl ester | 32.316 | 7.53 |
| 9 | Heptadecanoic acid, 14-methyl-, methyl ester | 32.468 | 3.52 |
| 10 | 8-Hexadecenal, 14-methyl-, (Z) | 32.695 | 2.41 |
| 11 | Trichloroacetic acid, undec-10-enyl ester | 32.930 | 2.88 |
| 12 | 2-Methyl-Z,3,13-octadecadienol | 33.447 | 3.70 |
| 13 | Cedran-8-ol, (8S,14) | 33.612 | 2.55 |
| 14 | 1,19-Eicosadiene | 22.792 | 2.27 |
| 15 | Tetracosamethyl-cyclododecasiloxane | 35.357 | 4.43 |
| 16 | Carbonic acid, but-3-en-1-yl eicosyl ester | 34.192 | 5.83 |
| 17 | Squalene | 38.529 | 4.36 |
| 18 | Hexanoic acid, heptadecyl ester | 35.865 | 2.65 |
| 19 | Heptasiloxane, hexadecamethyl | 40.956 | 1.62 |
| 20 | Bis(2-ethylhexyl) phthalate | 35.295 | 1.86 |
| 21 | 2(1H)-Naphthalenone, octahydro-4a-methyl-7-(1-methylethyl)- | 34.074 | 1.36 |

TGGATGAACCAGGAGCCATCCTTT. For GPX1, the forward primer was CGCTCTTTACCTTCTCGCGAA and the reverse primer was AGTTCAGGCAATGTCGTTGCGT.

Relative gene expression was measured with real-time PCR using the Qiagen Rotor-Gene Q 5plex HRM system with SYBR Green dye (Thermo Scientific, USA). GAPDH was used as the reference gene. Ct values for each target gene were normalized to GAPDH Ct values, and each reaction was performed in triplicate. Each qRT-PCR reaction contained 2 µL (200 ng) of cDNA, nuclease-free water, 5 µM of each primer, and 12.5 µL of SYBR Green Master Mix. ΔCt values were calculated by subtracting the GAPDH Ct from the mean Ct of the target genes (HSP90 and GPX1). ΔΔCt values were calculated by subtracting the ΔCt of the calibrator from that of the sample, and fold changes were determined using the 2^{-ΔΔCt} method. Gene expression levels in treated samples were compared, with all assays performed in triplicate.

2.10. ADMET and quantitative structure-activity relationship (QSAR) of bioactive compound

The bioactive compounds analyzed in this study were derived from extracts of the sea cucumber *H. lessoni*. Compound identification was performed using GC–MS, and the SMILES notation for each detected compound was retrieved from the PubChem database (NCBI, USA). Drug-likeness, pharmacodynamic properties, and toxicity profiles were evaluated for each ligand following Lipinski's Rule of Five (Lipinski et al., 2001). These assessments were conducted using ADMETLab 2.0 (Center for Drug Discovery and Development, Shanghai Jiao Tong University, China) and Protox 3.0 (Institute of Molecular Biology and Biophysics, Charité–Universitätsmedizin Berlin, Germany), with SMILES serving as the primary input for both platforms. The ADMET evaluation demonstrated that most compounds possessed favorable pharmacokinetic and pharmacodynamic characteristics, although several exhibited potential toxicity when considered as isolated compounds.

H. lessoni compounds that successfully passed the ADMET screening were subsequently evaluated for their potential using the Way2Drug PASS Online prediction tool (Way2Drug Group, Institute of Biomedical Chemistry, Moscow, Russia). This evaluation focused on determining their capacity to support IVF and IVM based on the Probability to Be Active (Pa) value. The Pa value was incorporated into the data-mining process because it indicates the predicted activity potential of each compound analyzed.

2.11. Prediction of protein targets and network analysis

Prediction of protein targets and gene–disease associations was carried out by analyzing protein targets using the SEA Search Server (Similarity Ensemble Approach; Keiser Laboratory, University of California San Francisco, USA), the Comparative Toxicogenomics Database (CTD; Mount Desert Island Biological Laboratory, USA), and Swiss Target Prediction (Swiss Institute of Bioinformatics, Switzerland), then comparing them with lists of proteins or genes associated with oxidative stress, endoplasmic reticulum stress, female infertility, oocyte maturation defects, and oocyte, zygote, and embryo maturation arrest from Open Targets (Open Targets Consortium, UK). This process produced a set of overlapping genes identified through Venn diagram analysis, which was visualized using JVenn (INRAE, France). The compiled protein targets were then entered into the STRING database (Search Tool for the Retrieval of Interacting Genes/Proteins; European Molecular Biology Laboratory, EMBL, Germany) with the organism set to *Homo sapiens*, network edges set to confidence, and the minimum required interaction score set to 0.900. The resulting network was exported in TSV format and further analyzed in Cytoscape (Institute for Systems Biology, Seattle, USA) to identify protein–protein interactions using degree, betweenness centrality and closeness centrality to determine the most influential proteins in the protein–protein interactions (PPI) network. Gene Ontology (GO) analysis using DAVID (Database for Annotation, Visualization and Integrated Discovery; National Institute of Allergy and Infectious Diseases, NIH, USA) showed that the potential protein targets of the sea cucumber extract play important roles in regulating ROS, oxidative stress, endoplasmic reticulum stress, as well as hormone regulation and cell growth. Meanwhile, the mechanisms of action of the bioactive compounds were identified using CTD and visualized in Cytoscape to map the modes of action relevant to IVF and IVM processes.

3. Results

3.1. GC–MS study

The GC–MS results (Table 1) demonstrate the high chemical complexity of the *H. lessoni* extract, consisting primarily of steroid- and ester-type compounds, along with minor amounts of glycerol detected at early retention times. Quantitatively, the major constituents were: propane, 1,2,2-trichloro-1,3,3,3-pentafluoro- (13.94 %); 9-octadecenoic acid (Z)-, 2,3-dihydroxypropyl ester (5.73 %); carbonic acid, but-3-en-1-yl eicosyl ester (5.83 %); phthalic acid, hexyl 1-phenylpropyl ester (5.87 %); and citronellal (3.04 %). Many of these compounds, particularly unsaturated fatty acids, fatty acid esters, squalene, and siloxane derivatives, have been reported to exhibit antioxidant, anti-inflammatory, or cytoprotective properties. This supports the hypothesis that *H. lessoni* extract may exert protective effects on embryo development, consistent with observations from other parts of this study.

3.2. In vitro study

The bar charts in Fig. 1 show the embryonic development of aged mouse oocytes at *H. lessoni* extract concentrations of 0 ppm (control), 15 ppm, 20 ppm, and 25 ppm. The y-axis represents extract concentration, while the x-axis shows the percentage of embryos formed. Both the 2-cell and blastocyst stages showed a fluctuating trend across the different concentrations with blastocyst formation consistently lower than the 2-cell stage. The 2-cell stage reached 83 % in the control group, declined to 71 % at 15 ppm, peaked at 100 % at 20 ppm, and then decreased to 89 % at 25 ppm. Blastocyst development, was 25 % in the control group (0 ppm) increasing slightly to 29 % at 20 ppm, and then fell sharply to 8 % at 25 ppm.

Fig. 2 shows embryonic development at extract concentrations of 0 (Fig. 2.1), 20 (Fig. 2.2), and 25 ppm (Fig. 2.3), focusing on two embryonic stages: the 2-cell stage and the blastocyst stage. Panel (a) shows embryos at the 2-cell stage (representing early post-fertilization cleavage) across all extract concentrations. In the control group (0 ppm; Fig. 2.1), a blastocyst is visible within the zona pellucida, exhibiting heterogeneous cytoplasm, a clearly defined blastocoel cavity, filled with transparent fluid. Embryos exposed to the extract, on the other hand, generally display blastomeres with more homogeneous cytoplasm. In the control, (0 ppm) the inner cell mass (ICM) appeared as a compact cluster of cells localized to one side, and partial protrusion of the blastocyst through the zona pellucida was evident, indicating the onset of

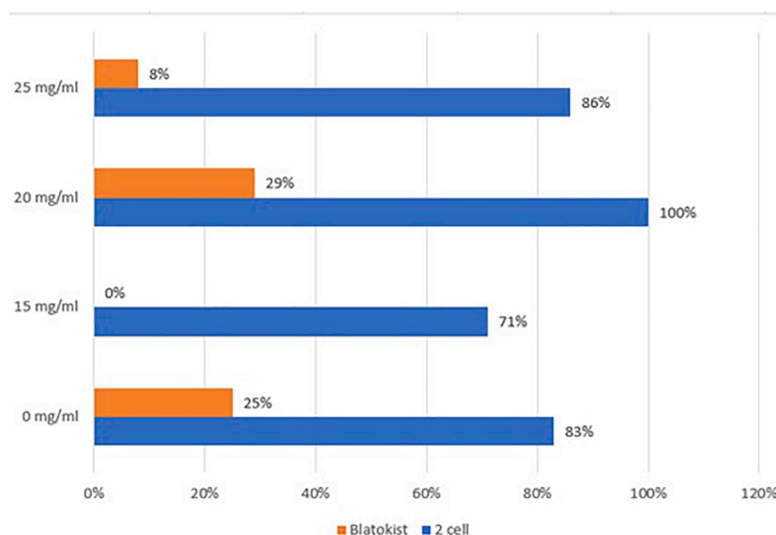


Fig. 1. Embryonic development of aged mouse oocytes at different *H. lessoni* extract concentrations. The bars represent the developmental competence of aged oocytes at different 2-cell and blastocyst embryonic stages following treatment at different concentrations (0 ppm, 15 ppm, 20 ppm, 25 ppm) of the tested extract.

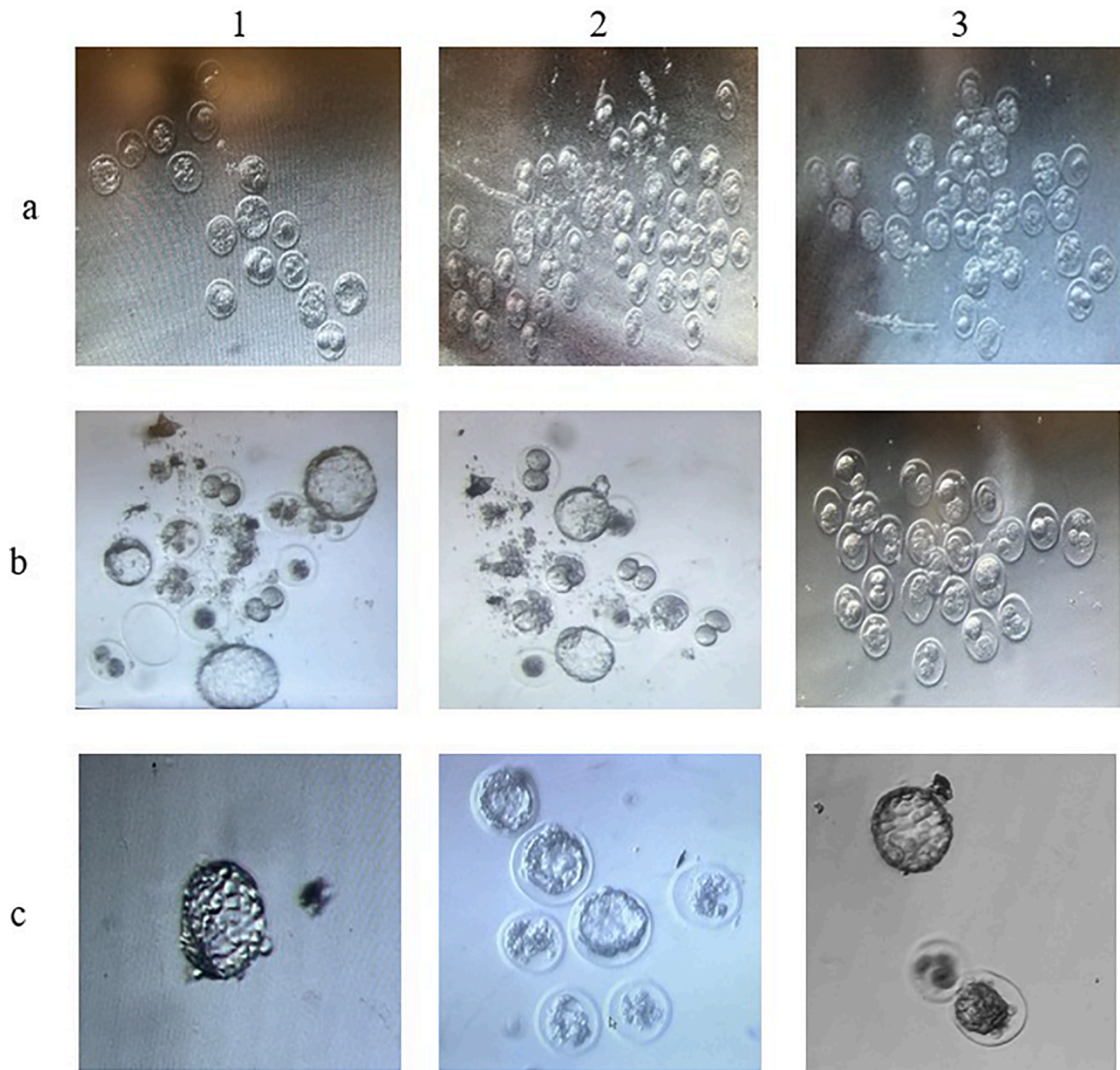


Fig. 2. Developmental competence of aged oocytes at different embryonic stages following treatment with various concentrations of the tested compound: 0 ppm (1), 20 ppm (2), and 25 ppm (3), and evaluated at different culture times: 24 h (a), 48 h (b), and 72 h (c).

hatching. A smaller blastocyst enclosed within an intact zona pellucida, was also visible, representing a slightly earlier developmental stage than the first.

At 15 ppm, embryos generally displayed good morphology, characterized by normal-shaped blastomeres, clear cellular structure, and relatively even cleavage patterns. Blastocysts showed a well-formed blastocoel cavity, an intact the zona pellucida with acceptable limits, and minimal cytoplasmic vacuolization, suggesting that a concentration of 15 ppm supports the maintenance of embryo developmental competence to an adequate level.

At 20 ppm (Fig. 2.2), several compact blastocysts showed densely arranged cells (located at the top left, centre left, and lower left of the panel) with little or no visible blastocyst cavity, and the ICM is not clearly distinguishable from the trophoblast. In partially expanded blastocysts, the blastocoel cavity begins to form and fill with fluid, the ICM becomes displaced towards one side, and the trophoblast cells are more clearly visible as a single cell layer. Overall, the blastocyst treated at 20 ppm show the most optimal morphology, with a wider and well-filled blastocoel cavity, more regular cell distribution, and a more clearly defined trophoblast (TE) and ICM.

Blastocysts treated at 25 ppm (Fig. 2.3) were examined four days after fertilization. The zona pellucida remained intact and clearly

defined. Although the blastocoel cavity had begun to form and contained cytoplasm, it was not yet fully expanded. Many blastomeres exhibited cytoplasmic vacuolization and increased granularity, with indications of cellular degeneration. At this highest concentration, most embryos only progressed to an early blastocyst stage, with a small cavity and uneven cell distribution. The ICM remained poorly defined, the TE appeared relatively thickened, and the overall morphology indicated impaired and delayed development (Table 2).

Blastocyst quality assessment was performed using the Gardner blastocyst grading system (Gardner et al., 2000), which includes

Table 2
Blastocyst position and gardner morphological grades.

| Image | Blastocyst Position | Stage | ICM Grade | TE Grade | Full Grade |
|-------|-------------------------|-------|-----------|----------|------------|
| 1c | Top (leading) | 3 | B | B | 3BB |
| 1c | Lower (2 cell) | 2 | C | C | 2CC |
| 2c | Higher-grade blastocyst | 3 | B | C | 3BC |
| 2c | Lower-grade blastocyst | 2 | C | C | 2CC |
| 3c | Top left | 3 | B | B | 3BB |
| 3c | Top right | 3 | B | C | 3BC |
| 3c | Lower | 3 | C | C | 3CC |

determination of blastocyst expansion (stage 1–6), ICM quality (A–C), and TE quality (A–C). These three parameters are then integrated into a composite score. Treatment with *H. lessoni* extract resulted in differences in blastocyst grade distribution at different extract concentrations. In the control group (0 ppm), blastocysts predominantly exhibited intermediate expansion (stage 2–3), with ICM and TE quality ranging from grades B to C. The most frequent composite scores were 3BC and 2CC, indicating blastocysts with a formed blastocoel cavity but reduced ICM integrity and a relatively sparse TE layer. This morphology is consistent with the limited developmental competence typically seen in aged oocytes without intervention.

The 20 ppm treatment group showed improved morphological quality according to the Gardner criteria. Most blastocysts reached stage 3 (expanded blastocyst) with ICM grade B and TE grades B–C, resulting in dominant composite scores of 3BB and 3BC. These findings suggest that moderate extract concentration not only increased the proportion of blastocysts formed, but also supported the development of a more compact ICM and a more organized TE layer compared with controls. In contrast, blastocyst quality declined at concentrations of 25 ppm. Most embryos remained at stage 2–3 with lower ICM and TE grades (ICM B–C and TE C), resulting in frequent low-quality composite scores such as single as 2CC, with only a single higher-grade 3BB blastocyst observed. These findings are consistent with evidence of cellular degeneration and morphological disruption at the highest concentration, reflected by reduced ICM and TE quality according to the Gardner criteria.

3.3. Effect of the extract on the mRNA expression levels of target genes

The effect of *H. lessoni* extract on relative mRNA expression of HSP90 and GPX1 in blastocysts shown in Fig. 3. Aged oocytes were subjected to *in vitro* maturation and fertilization in the presence of *H. lessoni* extract at concentrations of 0 ppm (control), 20 ppm, or 25 ppm, and embryos were cultured to the blastocyst stage. Total RNA was isolated from resulting blastocysts, reverse-transcribed into cDNA, and analyzed using qRT-PCR. Each reaction contained 200 ng of cDNA, and expression levels of HSP90 and GPX1 were normalized to the housekeeping gene GAPDH. At 20 ppm, both HSP90 and GPX1 were markedly upregulated, whereas at 25 ppm, GPX1 expression increased further while HSP90 expression declined to below baseline levels.

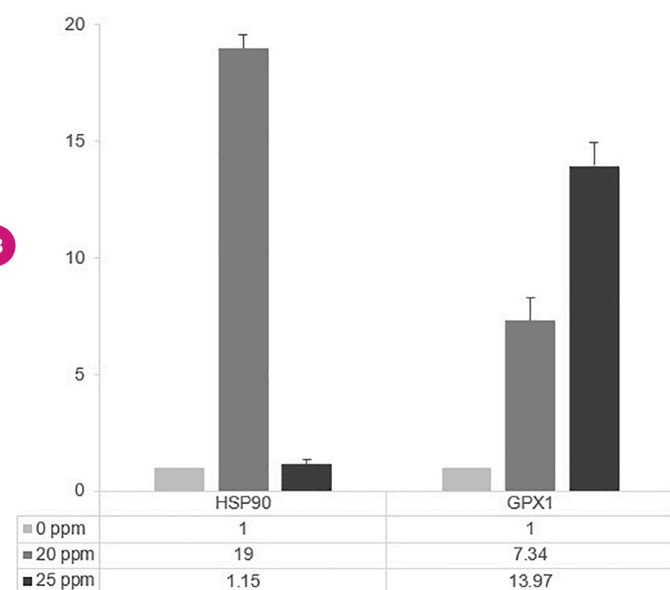


Fig. 3. Effect of *H. lessoni* extract on relative mRNA expression of HSP90 and GPX1 in blastocysts. Bars represent fold change in gene expression relative to the untreated control group (set to 1-fold).

3.4. In silico study

3.4.1. ADMET and QSAR of bioactive compound

The analysis showed that 18 of 20 *H. lessoni* bioactive compounds met Lipinski's Rule of Five, including limits for molecular weight, LogP, hydrogen bond donors and acceptors, and TPSA. ADMET results indicated that most compounds had good pharmacokinetic and pharmacodynamic properties. However, some showed potential liver toxicity or carcinogenic risks, and Pyrrolo[1,2-a]pyrazine-1,4-dione, hexahydro was classified as toxicity class 3. Based on these safety concerns, three compounds were excluded: Pyrrolo[1,2-a]pyrazine-1,4-dione, hexahydro; Tetracosamethyl-cyclododecasiloxane; and Heptasiloxane, hexadecamethyl (Table 3).

The bioactive potential of *H. lessoni* compounds was evaluated using the Way2Drug PASS tool. A Pa value above 0.3 indicates that a compound may support IVF procedures due to its strong structural similarity to database compounds known to produce related therapeutic effects (Fig. 4). Ten compounds showed average Pa values greater than 0.3 (green–yellow). The Pa score reflects the predicted activity of each tested compound and is determined by comparing the structure of the input compound (from the *H. lessoni* extract) with compounds previously confirmed to provide specific treatment effects, either through computational prediction (Pa > 0.3) or experimental validation (Pa > 0.7). Based on these predicted activities, the *H. lessoni* compounds appear to have strong potential as female anti-infertility agents, antioxidants, free-radical scavengers, oxygen scavengers, nitric oxide scavengers, and peroxidase inhibitors.

3.4.2. Prediction of protein targets and network analysis

The predicted target proteins of sea cucumber compounds from the SEA Target, CTD, and Swiss Target databases were compared with proteins linked to several stress conditions and reproductive disorders from the Open Target database. Venn analysis found six shared proteins also confirmed, namely NFE2L2, HSF1, HSP90AA1, HSP90B1, HSP90AB1, and GPX1. Another 2430 proteins overlapped between the predicted targets and open target database (Fig. 5).

In the graph topological network analysis, we used the overlapping proteins from the Venn diagram and processed them through the STRING server. The network analysis applied several variables that

Table 3
Results of drug-likeness and ADMET analysis of potential compounds.

| Compound Name | Lipinski | LD50 (mg/kg) | Toxicity Class |
|---|----------|--------------|----------------|
| Cyclodecanone | Accepted | 5000 | 5 |
| Propane, 1,2,2-trichloro-1,3,3,3-pentafluoro- | Accepted | 5000 | 5 |
| Phthalic acid, hexyl 1-phenyl propyl ester | Accepted | 29,600 | 6 |
| Citronellal | Accepted | 2420 | 5 |
| 3,6-Octadien-1-ol, 3,7-dimethyl-, (Z) | Accepted | 4700 | 5 |
| 9-Octadecenoic acid (Z)-, 2,3-dihydroxypropyl ester | Accepted | 39,800 | 6 |
| Heptadecanoic acid, 14-methyl-, methyl ester | Accepted | 5000 | 5 |
| 8-Hexadecenal, 14-methyl-, (Z) | Accepted | 5000 | 5 |
| Trichloroacetic acid, undec-10-enyl ester | Accepted | 5000 | 5 |
| 2-Methyl-Z,3,13-octadecadienol | Accepted | 1016 | 4 |
| Cedran-8-ol, (8S,14) | Accepted | 2000 | 4 |
| 1,19-Eicosadiene | Accepted | 5050 | 6 |
| Carbonic acid, but-3-en-1-yl eicosyl ester | Accepted | 5000 | 5 |
| Squalene | Accepted | 5000 | 5 |
| Hexanoic acid, heptadecyl ester | Accepted | 5000 | 5 |
| Bis(2-ethylhexyl) phthalate | Accepted | 1340 | 4 |
| 2(1H)-Naphthalenone, octahydro-4a-methyl-7-(1-methylethyl)- | Accepted | 500 | 4 |
| Pyrrolo[1,2-a]pyrazine-1,4-dione, hexahydro- | Accepted | 210 | 3 |
| Tetracosamethyl-cyclododecasiloxane | Rejected | 1540 | 4 |
| Heptasiloxane, hexadecamethyl | Rejected | 1540 | 4 |

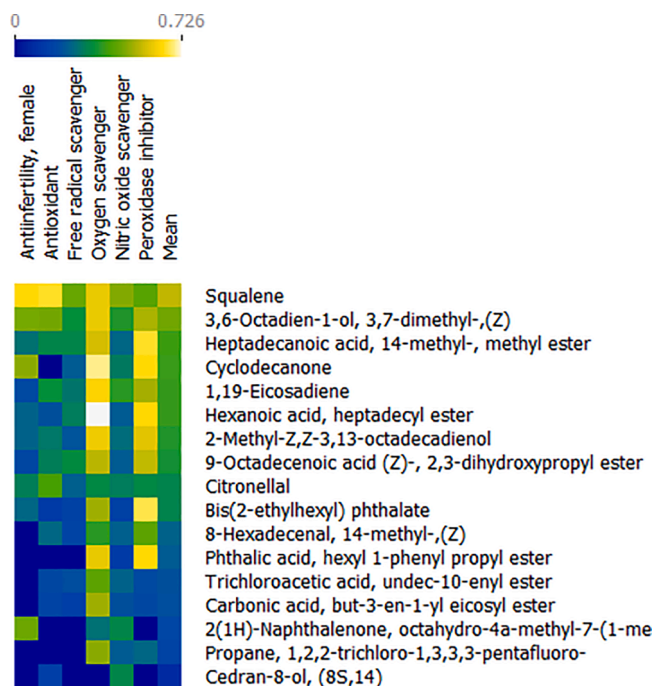


Fig. 4. Quantitative Structure-Activity Relationship Analysis of Bioactive Compound. The heatmap shows the correlation between various chemical compounds (right) and different biological activities (top). The color scale represents correlation strength, ranging from low (blue) to high (yellow).

describe the PPIs. These variables included Degree, Betweenness Centrality, and Closeness Centrality. The analysis showed that 209 potential proteins were involved in PPIs with a minimum required interaction score of 0.900 (highest confidence) (Fig. 6a). Based on betweenness centrality, the top 20 most promising protein targets were further identified (Fig. 6b).

The GO annotation of the most promising target proteins and genes was analyzed to determine their functions and their roles in pathways associated with IVF treatment. Only functional and pathway annotations with a False Discovery Rate (FDR) < 0.05 were included. An FDR of 0.05 indicates that up to 5% of the statistically significant results may be false positives. The GO analysis showed that the potential sea cucumber target genes play key roles in biological processes related to ROS regulation, oxidative stress, endoplasmic reticulum stress, hydrogen peroxide, nitric oxide, redox balance, and hormone regulation, including estradiol and estrogen (Fig. 7).

These potential proteins are also involved in growth-related processes such as embryonic placenta development, cell differentiation, and the mitotic cell cycle. When comparing target proteins, HSP90AA1, HSP90AB1, HSP90B1, BCL2, HSPA1A, HSPA1B, JUN, NFE2L2 (Nrf2), AKT1, EGFR, ESR1, and GPX1 were identified as the most frequently involved and dominant proteins in IVF and IVM treatment (Fig. 8).

Based on key roles in BP, CC, MF, and KEGG pathways for IVF and IVM, we identified 18 proteins that directly interact with the most promising compounds from *H. lessoni* extract. These proteins fall into four groups: oxidative stress protection, antioxidant defense, cell survival, and implantation and growth signaling. We also mapped their mechanisms of action with four matching compounds. Among these compounds, bis (2-ethylhexyl) phthalate (DEHP) shows the strongest potential by activating HSP90AA1, HSP90AB1, HSP90B1, GPX1, and NFE2L2. Citronellal, Squalene, and 2-Methyl-Z,Z-3-13-octadecadienol also provide protective effects by regulating BCL2, AKT1, and ESR1 (Fig. 9).

4. Discussion

GC-MS analysis revealed that extract of the sea cucumber *H. lessoni* is rich in unsaturated fatty acids, squalene, organosilicon derivatives, and other compounds with reported antioxidant and cytoprotective properties, supporting its potential to counteract age-related oxidative stress in oocytes and embryos. Concentration at 20 ppm significantly improved early cleavage, blastocyst formation, and overall embryo morphology relative to controls, whereas higher concentrations in 25 ppm caused degeneration and reduced developmental rates, indicating a bell-shaped dose-response effect. These findings align with previous observations that moderate antioxidant exposure enhances embryo quality, whereas excessive antioxidant stimulation can become detrimental.

The findings of this study demonstrate that *H. lessoni* extract modulates the developmental competence and stress-response profile of aged murine oocytes in a dose-dependent manner. The present findings are consistent with previous reports showing that marine-derived extracts and individual marine lipids can improve oocyte and embryo quality by attenuating oxidative stress and modulating apoptotic signaling in mammalian reproductive models (Khalilzadeh et al., 2016; Yu et al., 2025). A similar dose-dependent effect has been reported for the antioxidant quercetin where supplementation was found to improve early embryogenesis but higher concentrations became neutral or detrimental (Nontunha et al., 2020). The observed increase in blastocyst quality and ICM and TE organization at the optimal extract concentration is also consistent with a previous study that showed how targeted antioxidant support enhanced blastocyst morphology and Gardner grading under oxidative stress conditions (Zhang et al., 2025). Moreover, up-regulation of stress-responsive chaperones and antioxidant enzymes has been repeatedly associated with improved embryo survival in aging oocytes under oxidative stress conditions, while dysregulated expression of these genes correlates with developmental arrest and apoptosis (Cao et al., 2022). Collectively, our findings are broadly in agreement with the existing literature and extend it by linking the GC-MS-defined phytochemical profile of *H. lessoni* extract to coordinated changes in morphology, blastocyst grading, gene expression, and in silico stress-related networks in aged mouse oocytes. The GC-MS profile indicates that the *H. lessoni* extract contains multiple compounds capable of scavenging ROS, stabilizing cellular membranes, and modulating inflammatory and apoptotic signaling, including unsaturated fatty acid esters, squalene, and steroid-like molecules (Ujianti et al., 2024; Zhang et al., 2022). In aged oocytes, which are characterized by elevated ROS levels, mitochondrial dysfunction, and impaired proteostasis, such compounds likely improve the intracellular redox environment, preserve organelle integrity, and reduce oxidative damage to DNA, lipids, and proteins. Fatty acid ester can be incorporated into mitochondrial membranes, where they modulate key anabolic signaling pathways promoting mitochondrial biogenesis via upregulation of transcriptional regulators such as PGC1- α , TFAM, and Nrf1 (L Wang et al., 2021). Squalene has been described as an antioxidant that directly scavenges free radicals, reduces intracellular ROS, and prevents H₂O₂-induced oxidative and DNA damage (Zhang et al., 2023). Collectively, these bioactive compounds likely act as ROS scavengers and membrane protectants, improving the intracellular redox environment, preserving mitochondrial and ER integrity, and limiting oxidative damage to DNA, lipids, and proteins in aging oocytes and embryos (Das, 2021).

The *in vitro* results showed that treatment at 20 ppm led to significant upregulation of both HSP90 and GPX1, whereas treatment at 25 ppm induced excessive GPX1 expression but was accompanied by a decrease in HSP90. This interpretation is consistent with the findings of Önay Uçar et al., who demonstrated that HSP90 helps cells survive by protecting them from stress (Önay Uçar et al., 2023). Additionally, Hu et al. reported that long-chain bases (LCBs) from sea cucumber reduced ER stress by targeting oxidative, UPR, and inflammatory pathways (Hu et al., 2017). In contrast, at an extract concentration of 25 ppm, the

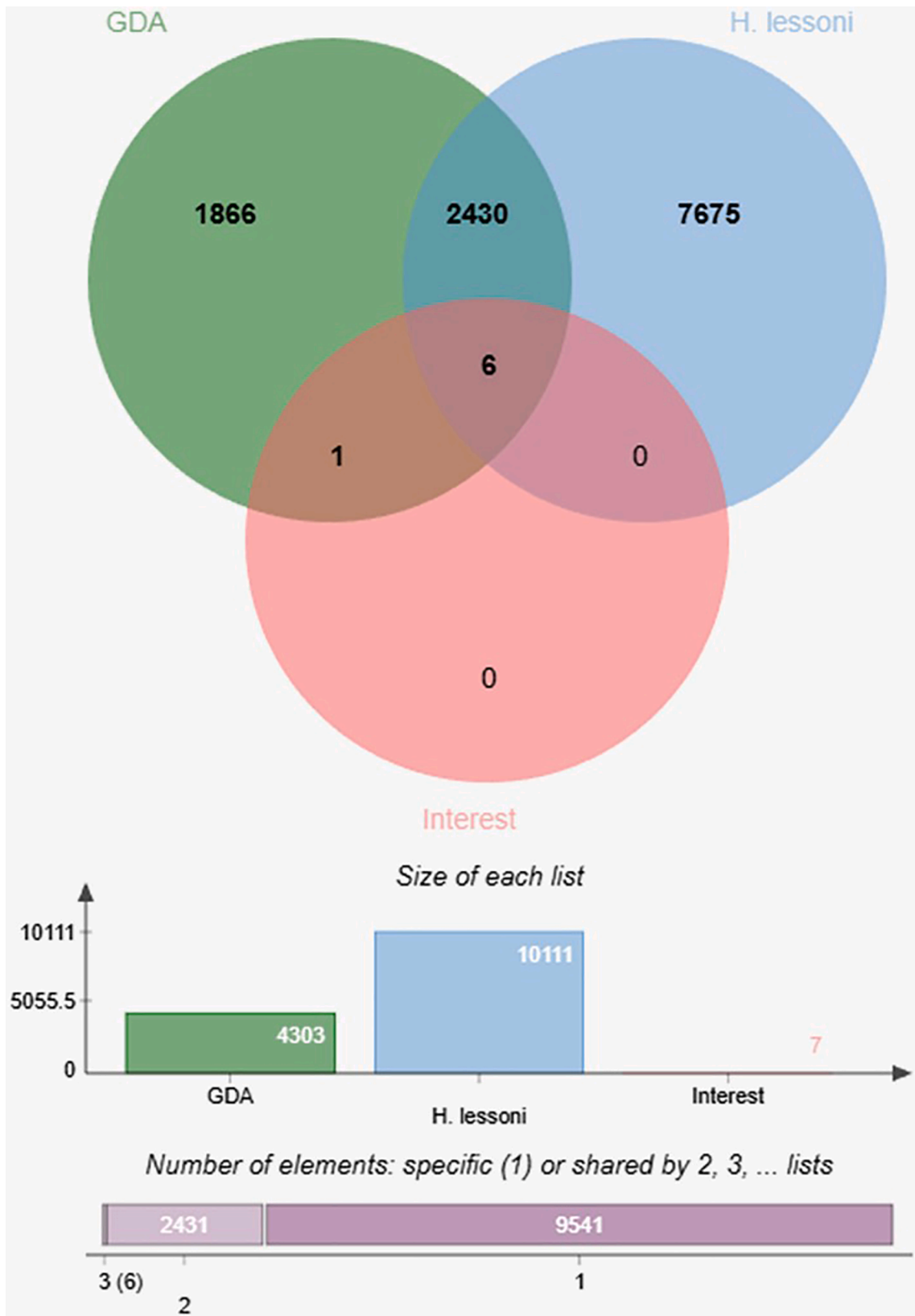


Fig. 5. Venn diagram and list-size comparison of predicted target proteins. The Venn diagram shows the overlap among protein targets from GDA, *H. lessoni* compound predictions, and proteins of interest. Six proteins were shared across all three datasets. The bar chart below displays the total number of proteins in each dataset.

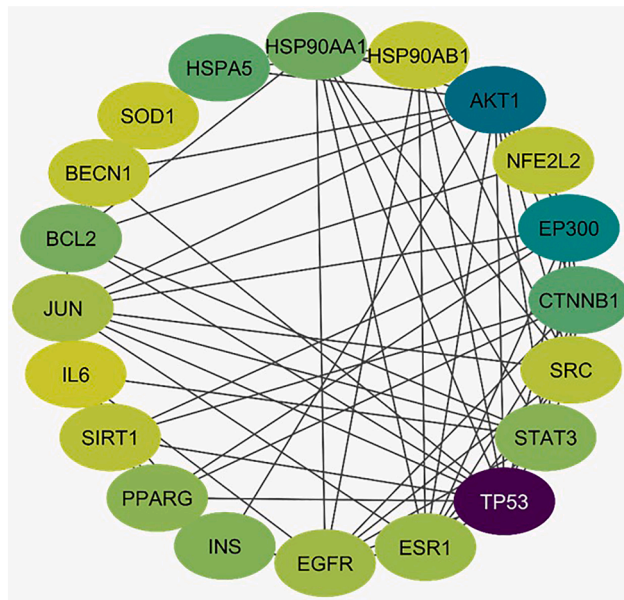
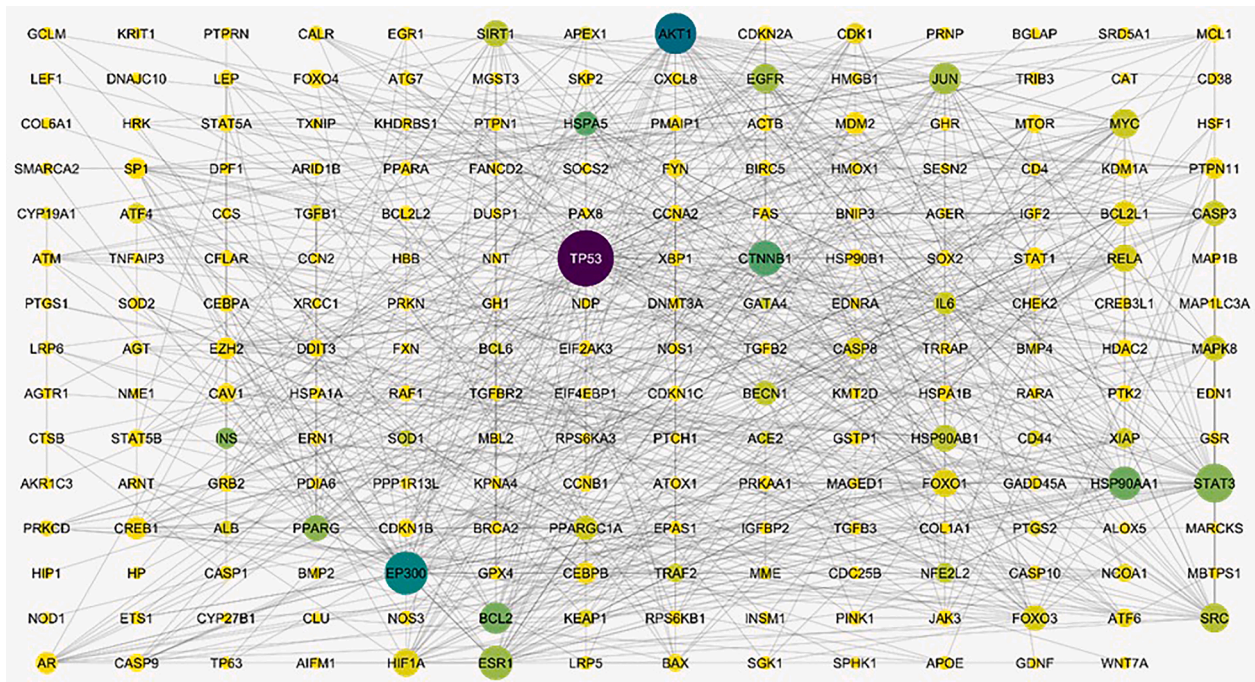


Fig. 6. Protein–protein interaction (PPI) networks of predicted sea cucumber bioactive compound targets linked to IVF and IVM. (a) Global STRING-based PPI network of 209 high-confidence protein targets, showing overall connectivity. Darker purple and larger nodes mark proteins with higher centrality. (b) Subnetwork showing the top 20 proteins ranked by betweenness centrality, highlighting their key roles in pathways related to oxidative stress, cell survival, and implantation.

molecular profile indicated a dysregulated stress response, in which increased GPX1 induction was not matched by sufficient chaperone capacity due to decreased HSP90 expression. This imbalance may promote the accumulation of misfolded proteins, prolong ER stress, and activate apoptosis, thereby compromising embryonic development beyond early cleavage (Ujianti et al., 2023). These molecular alterations are reflected in the marked reduction in blastocyst formation rate, deterioration of blastocyst morphology, and Gardner grading at the highest dose.

Among the compounds analyzed, bis(2-ethylhexyl) phthalate (DEHP) showed the strongest predicted activity. DEHP activates HSP90 family proteins, which help stabilize proteins required for spindle formation, cell cycle regulation, and stress resistance (Abd El-Fattah et al., 2016; Hou et al., 2022). It also activates GPX1 and NFE2L2 (Nrf2), major regulators of antioxidant defense, suggesting that DEHP helps protect

oocytes from oxidative and protein-related stress (J Wang et al., 2021). DEHP acts as an indirect antioxidant by triggering several protective molecular pathways highlighted in the network. DEHP strongly activates HSP90 proteins, which maintain proteostasis by stabilizing client proteins during oxidative stress and supporting survival pathways involving AKT1 and BCL2. Through these interactions, DEHP helps preserve mitochondrial integrity and reduce ROS-induced damage. It also stimulates the Nrf2 pathway, increasing expression of key antioxidant enzymes such as GPX1 and HMOX1, which lower peroxide levels and protect mitochondrial membranes (Chen et al., 2023).

In addition, DEHP shows strong connections with major regulators of the UPR and ER stress. Central nodes such as HSP90AA1, HSP90AB1, HSP90B1, HSPA5, and HSPA1B are essential ER chaperones involved in managing misfolded proteins (Melikov and Novák, 2024). This suggests that reducing oxidative stress may also decrease the accumulation of

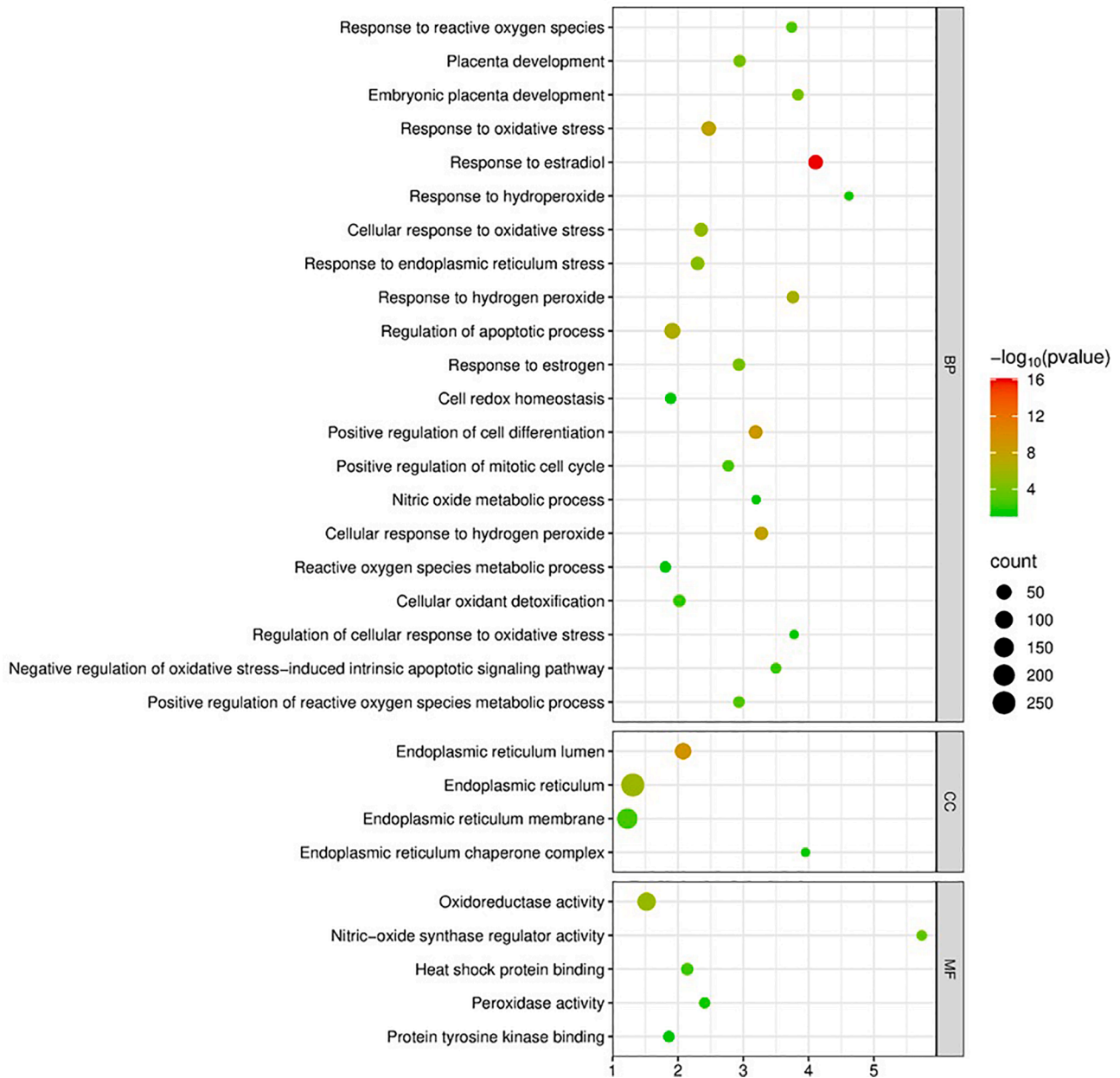


Fig. 7. Gene Ontology (GO) annotation of the most potential sea cucumber target proteins associated with IVF and IVM treatments. Enriched Biological Process (BP), Cellular Component (CC), and Molecular Function (MF) categories were identified.

misfolded proteins, thereby relieving ER stress and stabilizing the UPR system (Ong and Logue, 2023). On the other hand, the bioactive compound squalene acts as a strong antioxidant, as shown in the quantitative structure analysis conducted in this in silico study. Squalene is connected to AKT1, an important regulator of cell survival. At the membrane level, squalene embeds in the lipid bilayer and absorbs singlet oxygen and other radicals. This prevents lipid peroxidation and protects mitochondrial and oocyte membranes, helping maintain organelle structure and function. Squalene also activates anti-apoptotic signaling through BCL2, reduces mitochondrial membrane damage, and limits ROS-induced cell death, adding another layer of protection (Li et al., 2024). Other compounds, such as citronellal and 2-methyl-Z, Z-3-13-octadecadienol, support cell survival and implantation signaling by regulating BCL2, AKT1, and ESR1 (Mahmud et al., 2022). These targets help prevent apoptosis, maintain oocyte viability, and support hormone-related functions during maturation.

Compared with other marine species, sea cucumbers contain

exceptionally high levels of triterpenoid saponins and sulfated polysaccharides, which exhibit strong antioxidant and membrane-protective activities. These compounds, which are rare or absent in most aquatic organisms, modulate ER stress, UPR signaling, and mitochondrial stability, helping to explain the superior bioactivity of *H. lessoni*. In addition, *H. lessoni* provides distinctive saponins and triterpenes that stabilize cellular membranes and lessen ROS-induced damage, while long-chain bases further reduce ER stress and inflammation. Together, these components restore redox balance and ER homeostasis, improving oocyte quality. Oocyte developmental competence relies on tightly regulated ER proteostasis and mitochondrial oxidative phosphorylation. ER stress disrupts spindle formation and chromosome alignment, whereas impaired mitochondrial function limits the ATP required for successful cleavage. This unique combination of bioactive molecules supports the observed benefits of 20 ppm *H. lessoni* extract on early cleavage, blastocyst development, and the regulation of stress-response genes, linking the species' chemical profile to its enhanced effects in IVF.

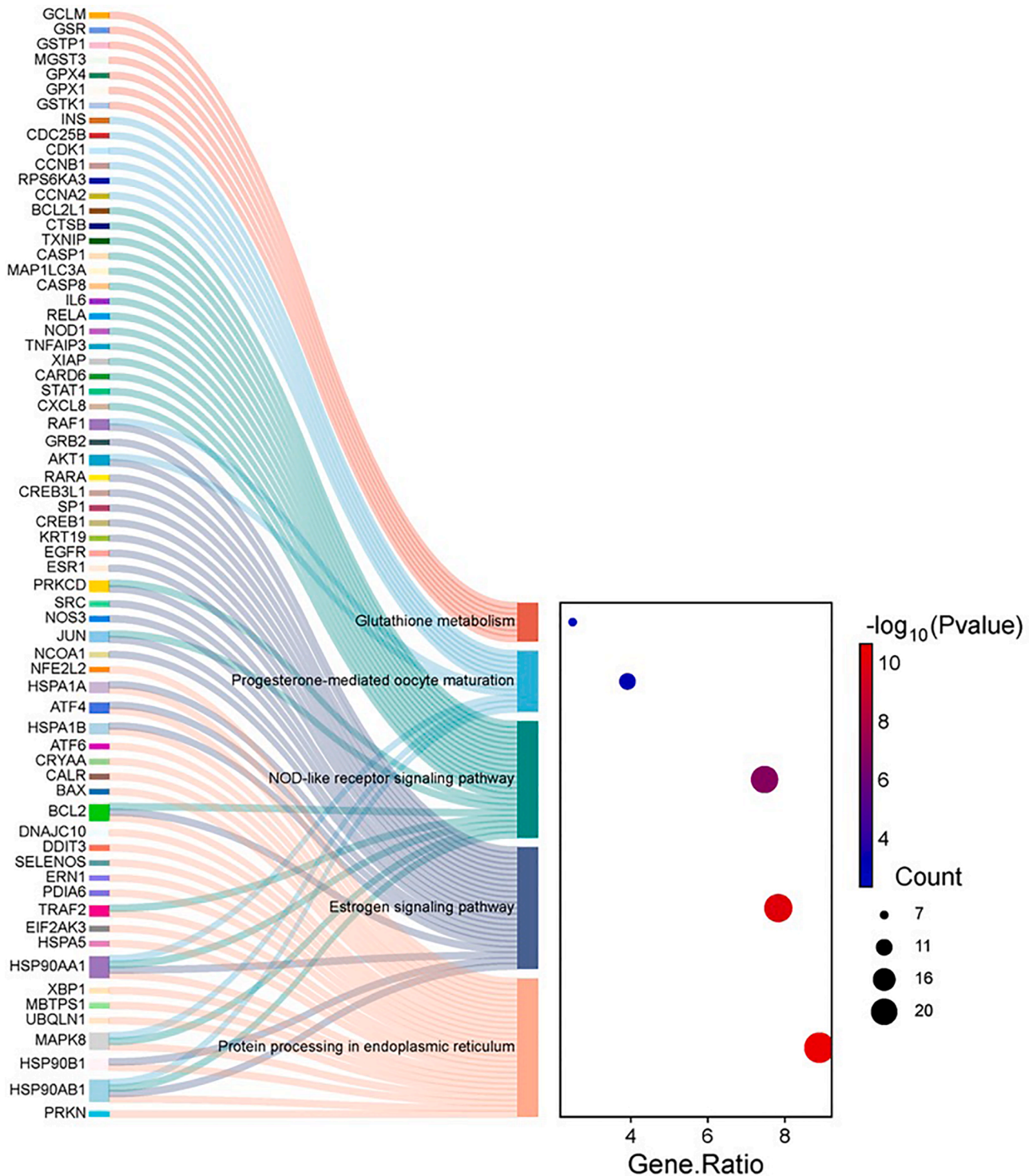


Fig. 8. Key protein targets identified. Proteins such as HSP90AA1, HSP90AB1, HSP90B1, BCL2, HSPA1A, HSPA1B, JUN, NFE2L2, AKT1, EGFR, ESR1, and GPX1 show major roles in processes linked to oxidative stress, cell survival, hormone signalling, and developmental competence, highlighting their value as indicators and molecular targets in IVF and IVM.

Accordingly, the observed changes in HSP90 and GPX1 expression reflect the molecular recovery of these two essential systems.

Although these findings position *H. lessoni* extract as a promising adjuvant to support aged oocytes in IVF settings, the limited improvement beyond early developmental stages suggests that additional interventions targeting mitochondrial function, spindle integrity, and chromosomal stability will be required to fully overcome age-related reproductive decline.

Funding

This study was financially supported by the Research Institute of Universitas Muhammadiyah Prof. Dr. Hamka, under contract number 594/F.03.07/2023.

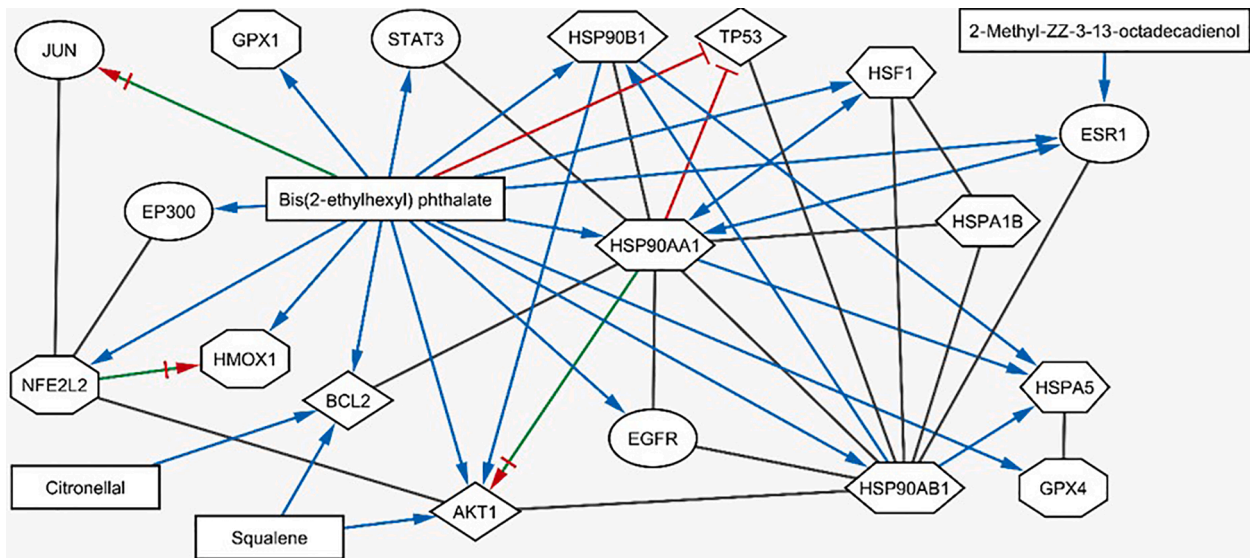


Fig. 9. Mechanism of action of *H. lessonii* extract compounds on proteins associated with IVF and IVM. Each protein is represented by a specific shape to indicate its biological function within the pathway: hexagon for oxidative stress protection, octagon for antioxidant defense, diamond for cell survival regulation, and ellipse for implantation and growth signal regulation. Blue arrows indicate activation or upregulation, red arrows indicate inhibition or downregulation, and green arrows denote potential regulatory effects on the corresponding protein targets.

CRediT authorship contribution statement

Irena Ujianti: Writing – original draft, Investigation, Conceptualization. **Mulyoto Pangestu:** Supervision, Investigation, Conceptualization. **Thomas Mayers:** Writing – original draft, Validation. **Wawang S Sukarya:** Project administration, Investigation, Funding acquisition. **Bety Semara Lakhsmi:** Data curation. **Zahra Nurushoffa:** Project administration. **Supandi:** Data curation. **Takashi Yashiro:** Project administration.

Declaration of competing interest

The authors declare that they have no known competing financial interests or personal relationships that could have appeared to influence the work reported in this paper.

Acknowledgements

We extend our heartfelt gratitude to the Faculty of Medicine at Universitas Muhammadiyah Prof. Dr. Hamka and Education Program in Development and Reproduction Laboratory, Faculty of Medicine, Monash University, Clayton, Australia for the generous support that enabled this research to be realized. We would also like to acknowledge and convey our appreciation to all individuals who have provided assistance throughout this research process.

References

Abd El-Fattah, A.A., Fahim, A.T., Sadik, N.A.H., Ali, B.M., 2016. Resveratrol and curcumin ameliorate di-(2-ethylhexyl) phthalate induced testicular injury in rats. *Gen. Comp. Endocrinol.* 225, 45–54. <https://doi.org/10.1016/j.ygcn.2015.09.006>.

Al'asyi, A., Ujianti, I., Nadika, R., Zahirah, Z., Faizin, B.J., Afifah, D.A., et al., 2025. Exploring the potential of *Holothuria atra* extract in modulating fasting triglyceride index and obesity: in silico, in vitro and in vivo studies. *Narra J.* 5, 2839. <https://doi.org/10.52225/narra.v5i3.2839>.

Askari, S., Jafarzadeh Shirazi, M.R., Ahmadi, M., Khoradmeh, A., Mussin, N.M., Kaliyev, A.A., et al., 2024. Impact of alcoholic extract from sea cucumber (*Holothuria parva*) on letrozole-induced polycystic ovary syndrome in adult female rats. *Asian Pac. J. Reprod.* 13, 261–270. <https://doi.org/10.4103/apjr.3.24>.

Broekmans, F.J., Soules, M.R., Fauser, B.C., 2009. Ovarian aging: mechanisms and clinical consequences. *Endocr. Rev.* 30, 465–493. <https://doi.org/10.1210/er.2009-0006>.

Cao, B., Qin, J., Pan, B., Qazi, I.H., Ye, J., Fang, Y., Zhou, G., 2022. Oxidative stress and oocyte cryopreservation: recent advances in mitigation strategies involving antioxidants. *Cells* 11, 3573. <https://doi.org/10.3390/cells11223573>.

Chen, M.S., Wang, J.X., Zhang, H., Cui, J.G., Zhao, Y., Li, J.L., 2023. Novel role of hemoxygenase-1 in phthalate-induced renal proximal tubule cell ferroptosis. *J. Agric. Food Chem.* 71 (5), 2579–2589. <https://doi.org/10.1021/acs.jafc.2c07762>.

Das, U.N., 2021. Cell membrane theory of senescence and the role of bioactive lipids in aging, and aging-associated diseases and their therapeutic implications. *Biomolecules* 11, 241. <https://doi.org/10.3390/biom11020241>.

Gardner, D.K., Lane, M., Stevens, J., Schlenker, T., Schoolcraft, W.B., 2000. Blastocyst score affects implantation and pregnancy outcome: towards a single blastocyst transfer. *Fertil. Steril.* 73, 1155–1158. [https://doi.org/10.1016/S0015-0282\(00\)00518-5](https://doi.org/10.1016/S0015-0282(00)00518-5).

Hoang Thanh, H., Liang, Q., Luo, X., Tang, Y., Qin, J.G., Zhang, W., 2022. Bioactives from marine animals: potential benefits for human reproductive health. *Front. Mar. Sci.* 9, 872775. <https://doi.org/10.3389/fmars.2022.872775>.

Hou, P., Dai, W., Jin, Y., Zhao, F., Liu, J., Liu, H., 2022. Maternal exposure to di-2-ethylhexyl phthalate (DEHP) depresses lactation capacity in mice. *Sci. Total Env.* 837, 155813. <https://doi.org/10.1016/j.scitotenv.2022.155813>.

Hu, S., Wang, J., Wang, J., Xue, C., Wang, Y., 2017. Long-chain bases from sea cucumber mitigate endoplasmic reticulum stress and inflammation in obesity mice. *J. Food Drug Anal.* 25, 628–636. <https://doi.org/10.1016/j.jfda.2016.10.011>.

Khalilzadeh, M., Baharara, J., Jalali, M., Namvar, F., Amini, E., 2016. The sea cucumber body wall extract promoted in vitromaturation of NMRI mice follicles at germinal vesicle stage. *Zahedan J. Res. Med. Sci.* 18, e3021. <https://doi.org/10.17795/zjrms-3021>.

Kunachowicz, D., Król-Kulikowska, M., Raczycka, W., Slezia, J., Błażejewska, M., Kulbacka, J., 2024. Heat shock proteins, a double-edged sword: significance in cancer progression, chemotherapy resistance and novel therapeutic perspectives. *Cancers* 16, 1500. <https://doi.org/10.3390/cancers16081500>.

Li, G., Chen, L., Bai, H., Zhang, L., Wang, J., Li, W., 2024. Depletion of squalene epoxidase in synergy with glutathione peroxidase 4 inhibitor RSL3 overcomes oxidative stress resistance in lung squamous cell carcinoma. *Precis. Clin. Med.* 7 (2), pbae011. <https://doi.org/10.1093/pmedi/pbae011>.

Lipinski, C.A., Lombardo, F., Dominy, B.W., Feeney, P.J., 2001. Experimental and computational approaches to estimate solubility and permeability in drug discovery and development settings. *Adv. Drug Deliv. Rev.* 46, 3–26. [https://doi.org/10.1016/S0169-409X\(00\)00129-0](https://doi.org/10.1016/S0169-409X(00)00129-0).

Ma, M., Zhang, L., Liu, Z., Teng, Y., Li, M., Peng, X., An, L., 2024. Effect of blastocyst development on hatching and embryo implantation. *Theriogenology* 214, 66–72. <https://doi.org/10.1016/j.theriogenology.2023.10.011>.

Mahmud, F., Mahedi, M.R.A., Afrin, S., Haque, R., Hasan, M.S., Sum, F.A., Kuri, O.C., 2022. Biological & insecticidal effect of citronella oil: a short review. *Clin. Med. Health Res. J.* 2 (6), 261–265. <https://doi.org/10.18535/cmhrj.v2i6.108>.

Maskur, M., Sayuti, M., Widyasari, F., Setiarto, R.H.B., 2024. Bioactive compound and functional properties of sea cucumbers as nutraceutical products. *Rev. Agric. Sci.* 12, 45–64. <https://doi.org/10.7831/ras.12.0.45>.

Melikov, A., Novák, P., 2024. Heat shock protein network: the mode of action, the role in protein folding and human pathologies. *Folia Biol.* 70 (3). <https://doi.org/10.14712/fb2024070030152>.

